

# Automatic Defect Detection and Grading of Single-Color Fruits Using HSV (Hue, Saturation, Value) Color Space

Saeideh Gorji Kandi

*Department of Color imaging & Color Image Processing, Institute for Color Science & Technology, Tehran, 16765-654, Iran*

Received: November 09, 2010 / Accepted: November 12, 2010 / Published: December 30, 2010.

**Abstract:** Machine vision has been recently utilized for quality control of food and agricultural products, which was traditionally done by manual inspection. The present study was an attempt for automatic defect detection and sorting of some single-color fruits such as banana and plum. Fruit images were captured using a color digital camera with capturing direction of zero degree and under illuminant  $D_{65}$ . It was observed that growing decay and time-aging made surface color changes in bruised parts of the object. 3D RGB and HSV color vectors as well as a single channel like H (hue), S (saturation), V (value) and grey scale images were applied for color quantization of the object. Results showed that there was a distinct threshold in the histogram of the S channel of images which can be applied to separate the object from its background. Moreover, the color change via the defect and time-aging is correctly distinguishable in the hue channel image. The effect of illumination, gloss and shadow of 3D image processing is less noticeable for hue data in comparison to saturation and value. The value of H channel was quantized to five groups based on the difference between each pixel value and the H value of a healthy object. The percentage of different degree of defects can be computed and used for grading the fruits.

**Key words:** Machine vision, HSV color space, fruit, grading, defect detection.

## 1. Introduction

Human visual inspection is tedious, time-consuming, laborious, non-consistent, and heavily dependent on the person's mood and easily changes based on physiological characteristics. During the last decades, developments in computer hardware and software have introduced objective methods for quality control in different industries.

Nowadays, machine vision systems provide with a real time cost effective, consistent, high-speed and accurate quality assessment of products [1]. Machine vision consists of two main parts, including image capturing and image processing that result in a non-contact and non-destructive opportunity for quality measurement. Furthermore, color is an important feature for quality assessments, which is extensively used for grading agricultural products. The

color correlates well with other physical, chemical and sensory properties and can be used to estimate ripeness, degree of defects, safety, storage time, nutritional value etc. [2]. Color machine vision and color image processing can result in color measurement, quality inspection and classification of food and agricultural products, and can yield significant savings in terms of labor costs together with an increase in product quality.

3D and color vision would accelerate machine vision development to obtain high accuracy that is needed in the industry [1,2]. As an example, some of these applications are listed here. Color image processing was applied to distinguish between good and green potatoes and between yellow and green 'Golden Delicious' apples. The proposed algorithm was claimed to have over 90% accuracy [3]. Grading tomatoes based on maturity stages was carried out using color machine vision [4]. It was reported that classification results agreed with manual grading in 77% of the tested tomatoes. A paper utilized

---

**Corresponding author:** Saeideh Gorji Kandi, Ph.D., assistant professor, research fields: color physics and color imaging. E-mail: sgorji@icrc.ac.ir.

image-processing techniques to convey and grade fruit products using a color CCD camera for external inspection and an X-ray sensor to detect biological defects [5]. Computer vision applied feature extraction and a neural network algorithm was performed for grading some vegetables such as strawberry and pepper [6]. Machine vision based on Principal Component Analysis technique was proposed for classification of sugar mango using physical properties of fruits, such as height, width, volume, weight, and maturity level [7].

A computer vision system was proposed for classification of olives based on their external appearance [8]. The introduced methodology made use of color parameters and morphological features. Another paper described a machine vision system for real-time color classification and sorting of a variety of agricultural products such as seeds, meat, baked goods, plant and wood [9]. Some studies applied color image processing for peach grading [10]. An image analysis system was developed to evaluate the color of stone fruits and real time maturity grading of fresh market peaches [11]. It was reported that manual grading differed from image analysis and colorimeter results for the late-season cultivars due to a less blushed surface.

A machine vision system was implemented to quantify standard color of fruit and vegetables [12]. Another digital image classification system based on Bayesian interference techniques was introduced to grade six types of fresh products [13]. It was reported that digital color image processing can be a powerful and low-cost tool for color grading of fruits.

The objective of the present study is to apply computer vision methods for defect detection and grading of some single-color fruits, especially banana and plum

## **2. Materials & Methods**

### *2.1 Materials*

A machine vision system was employed for defect detection and grading of some single-color fresh fruits

such as banana and golden plum. The bananas and golden plums were from Bam and Baraghan of Iran respectively. They were got from market and were ripe. For this purpose, the following procedure was implemented.

### *2.2 Image Acquisition*

One of the most important factors having influence on the quality of captured images and the performance of image processing is the illumination. In this research, D<sub>65</sub> standard illuminant which is a simulation of daylight source was applied. After applying different illuminating setups, a diffuse illumination was preferred instead of direct illumination.

A Canon EOS 500D digital color camera with EF-S 18-55 mm f/3.5-5.6 lens (Canon INC., Japan) was used for image capturing. The camera was set on autofocus and a white heavy coated paper with an  $L^*$  value of about 95 was used for white balancing. The camera was located over the sample at the distance of 50 cm. The angle between the sample and the camera was adjusted to zero. A matte black surface was taken as background. Images were stored in JPEG format using high quality level, and the camera was connected to the USB port of a computer provided with a Remote Capture Software to monitor and acquire images.

### *2.3 The Proposed Method*

#### *2.3.1 Color Space*

The color space used by the camera is optionally sRGB or Adobe RGB. It is well known that other color spaces such as CIE 1976  $L^*a^*b^*$  and HSV correlate better with human visual perception and might be resulted better for introducing a machine vision system instead of human detection. The CIE 1976  $L^*a^*b^*$  space, abbreviated as “CIELAB”, was intended for equal perceptual differences for equal changes in the coordinates  $L^*$ ,  $a^*$  and  $b^*$ . It is used intensively in many industries and provides a standard scale for comparison of color values. The CIELAB coordinates ( $L^*$ ,  $a^*$ ,  $b^*$ ) can be calculated from the tristimulus values X, Y and

Z. The tristimulus values, X, Y and Z of the samples can be computed with the following formulas:

$$\begin{aligned} X &= \sum_{\lambda} \bar{x}_{\lambda} \cdot e_{\lambda} \cdot R_{\lambda} \\ Y &= \sum_{\lambda} \bar{y}_{\lambda} \cdot e_{\lambda} \cdot R_{\lambda} \\ Z &= \sum_{\lambda} \bar{z}_{\lambda} \cdot e_{\lambda} \cdot R_{\lambda} \end{aligned} \quad (1)$$

Where  $\bar{x}$ ,  $\bar{y}$  and  $\bar{z}$  are the CIE color matching functions,  $e$  presents the spectral power distribution of the illuminant and  $R$  is the spectral reflectance of the samples. The equations for CIELAB color space are as follows [14, 15]:

$$\begin{aligned} L^* &= 116 f\left(\frac{Y}{Y_n}\right) - 16 \\ a^* &= 500 \left[ f\left(\frac{X}{X_n}\right) - f\left(\frac{Y}{Y_n}\right) \right] \\ b^* &= 200 \left[ f\left(\frac{Y}{Y_n}\right) - f\left(\frac{Z}{Z_n}\right) \right] \end{aligned} \quad (2)$$

Where  $X_n$ ,  $Y_n$  and  $Z_n$  are the tristimulus values of the reference white. The  $L^*$ ,  $a^*$  and  $b^*$  present lightness, redness-greenness and yellow-blueness, respectively. Fig. 1 shows a schematic form of this color space.

The CIELAB color coordinates can also be expressed in cylindrical coordinates with chroma  $C_{ab}^*$  and hue  $h_{ab}$ . The  $C_{ab}^*$  axis represents chroma or saturation, which is obtained as a distance between the origin (center or achromatic axis of CIELAB color space) and the point expressed by the coordinates  $a^*$  and  $b^*$  according to Eq. (3). Higher saturated color represents higher chroma value and is closer to the edge of the circle and vice versa.

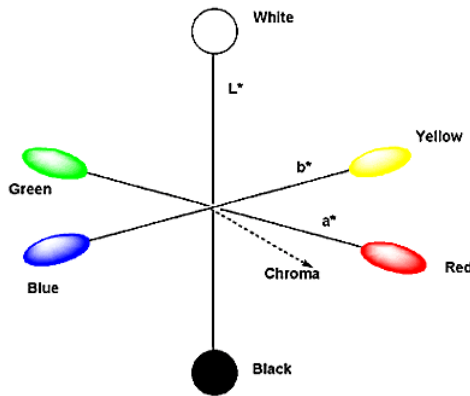


Fig. 1 A schematic form of CIELAB 1976 color axis.

$$C_{ab}^* = (a^{*2} + b^{*2})^{1/2} \quad (3)$$

The CIE 1976 hue angle ( $h_{ab}$ ) is obtained by the following equation.

$$h_{ab} = \tan^{-1}\left(\frac{b^*}{a^*}\right) \quad (4)$$

Where  $h_{ab}$  lies between  $0^\circ$  and  $360^\circ$  based on signs of  $a^*$  and  $b^*$  [14, 15].

If camera storage is set as sRGB,  $L^*a^*b^*$  and HSV measures can be estimated by standard equations and for this Matlab software was used. Application of different color spaces showed that HSV color space is appropriate for the purpose of this research. This is discussed in the next section.

### 2.3.2 Background Removal

At first, it was necessary to remove the background from the image. Evaluating the captured images showed that because of implementing a black background, the histogram of the image in saturation channel gives a distinct threshold between the object and background which can be precisely used for background detection. Fig. 2 shows an S channel histogram of a captured image. As illustrated, the first part of the histogram which is related to the background can be feasibly separated from the object. In the other way the background was a black surface which was constant for each image. Different captured images showed that the S values of the background was less than 0.3, therefore it was simply used as threshold value to separate the background from the object.

### 2.3.3 Defect Detection and Grading

Since the defects and aging usually appeared in the

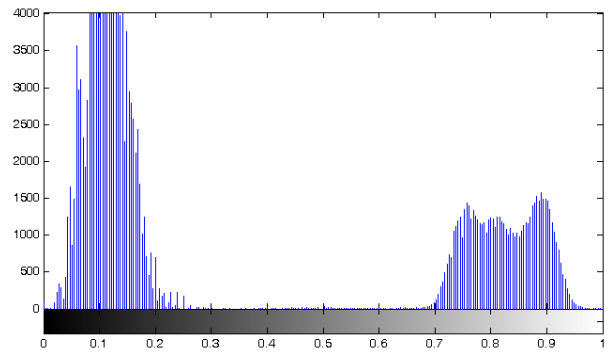


Fig. 2 The histogram of the S channel of a captured image.

color of the object, it can be useful to segment the object based on its color.

During preliminary experiments, image segmentation in sRGB color space was tested applying some clustering methods. The obtained results were not acceptable, which was mainly because of the lighting effect which imposed glossy parts on the object. Different subparts of a sample which was expected to be grouped in a single cluster belonged to different groups because of illuminating effects. Therefore, it was not possible to separate the decayed parts from sound ones. After evaluating each channel of the image (including H, S and V) separately, it was found that the color change because of the defects and aging could be classified in H channel properly. Using the H channel data, the effect of lighting condition, camera position and irregularity of the object (which is the most important one) on the captured image almost disappeared. It might be these parameters have definite effect on the lightness of the image which can be observed in the S and V channels.

Therefore, at first the images were converted to HSV color space and then the data of the H channel was

assessed. To be able to grade the object based on H values it is necessary to get a standard value and compare the other measures with it. It can be easily done by a calibration step in which the standard value for each kind of fruit can be obtained by a preliminary experiment. To do that, a healthy and completely acceptable fruit is to be selected. The image of the sample is captured and converted to HSV space. The mean of pixel values in H channel is applied as the standard value. Fig. 3 shows an example, a healthy sample which is segmented from its background (the background is black), together with the H channel image and the histogram of it. As expected, the H histogram of the sample has a sharp Gaussian shape, and it can be used as the dominant H value for this type of banana. It should be noted that this standard value can be also achieved by applying a set of healthy samples and averaging their obtained results.

Then, the sample image should be segmented considering the standard value which was obtained from the last step. It is possible to segment the images by thresholding the histogram of H channel. To do that, the standard value is set as the center, and then the H

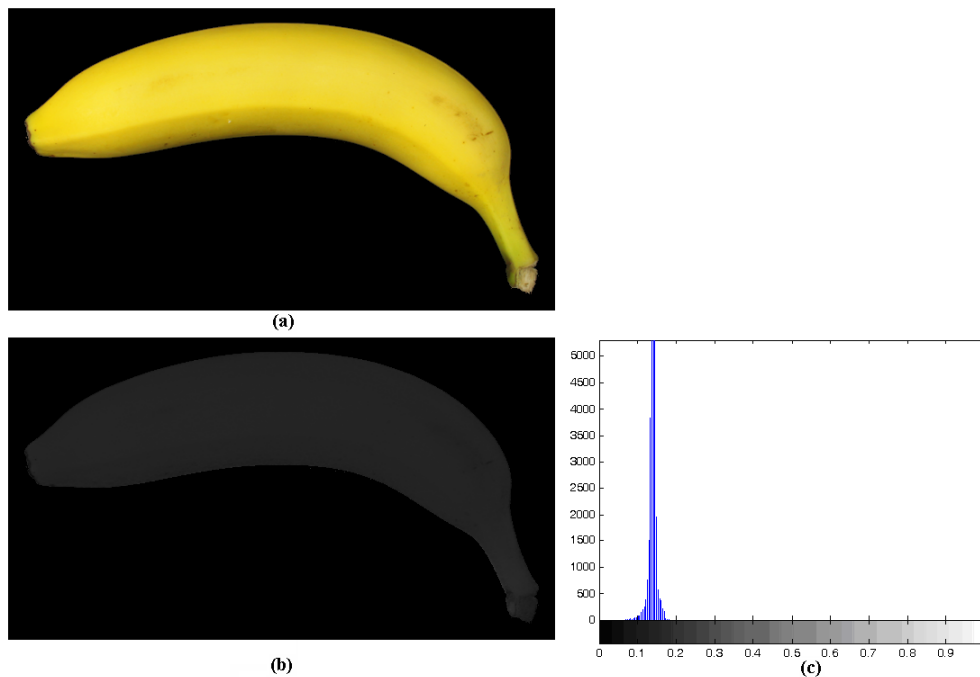


**Fig. 3** (a) The image of a banana which is separated from its background; (b) the hue channel of (a); (c) the histogram plot of hue channel.

value difference between each pixel value and the center is computed by equation (5).

$$\Delta h_i = |h_i - h_s| \quad (5)$$

where  $h_i$  indicates the  $h$  value of the  $i$ th pixel and  $h_s$  represents the standard  $h$  value.

The quantization process is applied considering the computed difference values in Table 1.

The values of  $\epsilon$  can be simply estimated for each type of fruit based on some experimental images. The quantization levels (1, 200/255, 150/255, 100/255, 50/255 and 0) were selected arbitrary with the distribution to have distinguishable parts in quantized image.

### 3. Results and Discussion

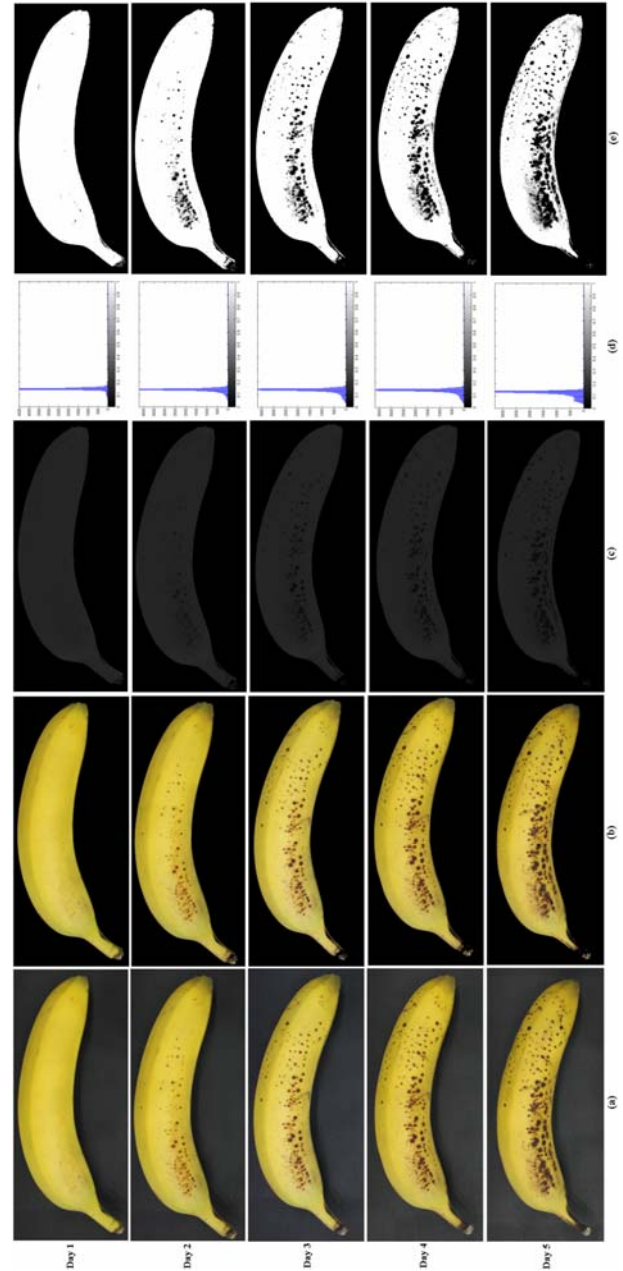
Fig. 4 shows the captured images of a banana during 5 days and the results of background removal, H channel images, the histogram of H channel and the segmented images. As demonstrated, aging and defect change the color of the samples. The part c of Fig. 4 shows that the color changes because the decays can be precisely distinguished in H channel. Comparing the part (e) with (a) or (b) indicates that the proposed method can segment the images based on the degree of the defects.

Table 2 indicates the percentage of each segment for the banana samples which can be applied for grading them.

Fig. 5 shows the images of a golden plum and the results of image quantization applying the proposed method during 6 days. It is demonstrated that the decay of plum images can be recognized in quantized images. Table 3 gives the percentage of each part.

**Table 1** The quantization levels based on  $h_i$  values.

$\Delta h_i$	$h_i$
$\leq \epsilon_1$	1
$> \epsilon_1 \ \& \ \leq \epsilon_2$	200/255
$> \epsilon_2 \ \& \ \leq \epsilon_3$	150/255
$> \epsilon_3 \ \& \ \leq \epsilon_4$	100/255
$> \epsilon_4 \ \& \ \leq \epsilon_5$	50/255
$> \epsilon_5$	0



**Fig. 4** The images of banana during 5 days together with the proposed method results.

(a): the original images in five days; (b): the images of 'a' after background removal; (c): the H channel of 'b'; (d): the histogram of 'c'; (e): the quantized images of 'c'.

**Table 2** The percentage of each segment for the images of Fig. 4.

Days	White	Grey 1	Grey 2	Grey 3	Black
3	84.96	6.29	2.50	1.58	4.67
4	78.51	9.51	3.38	1.86	6.74
5	68.03	13.73	5.45	3.16	9.63

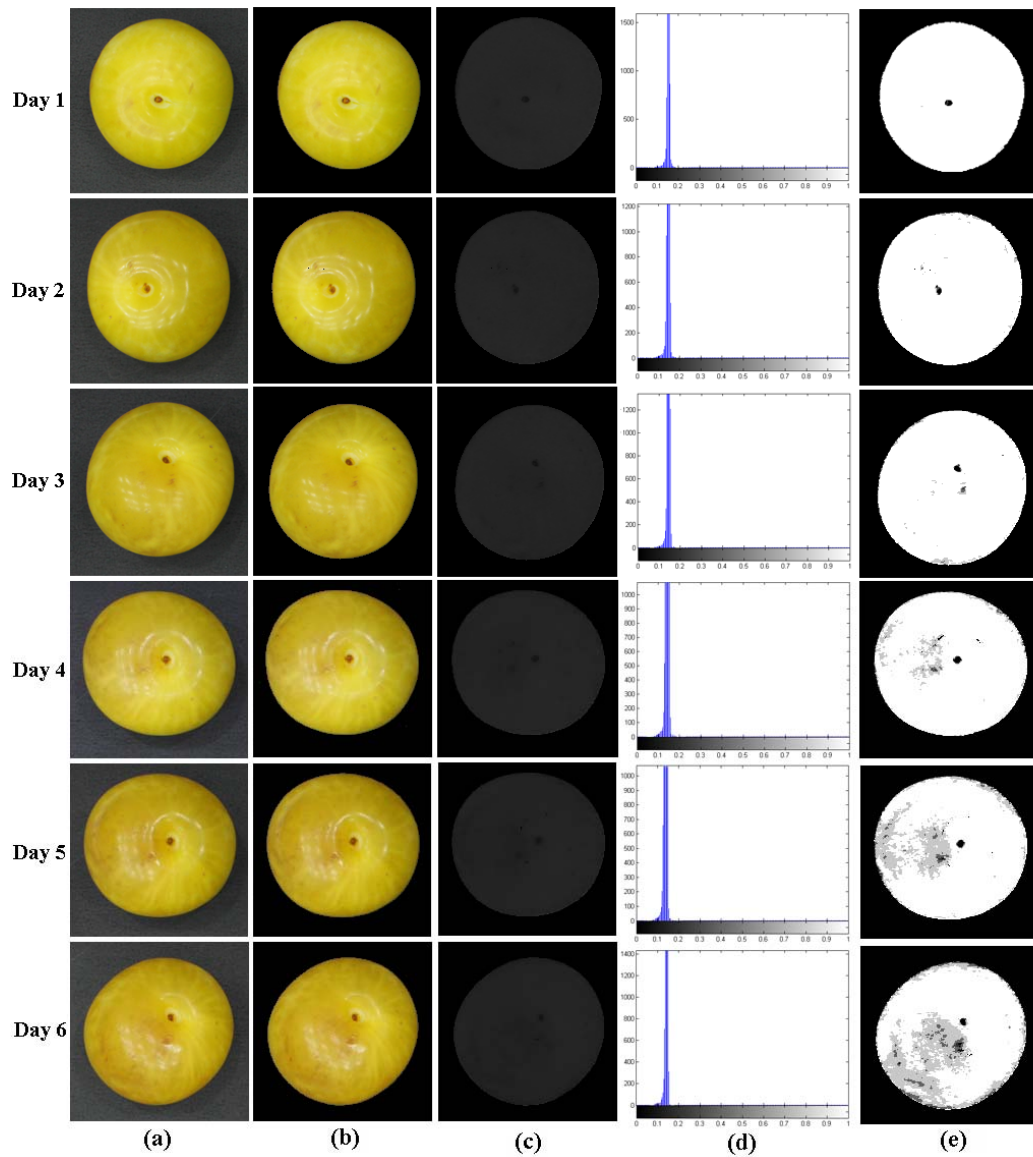


**Fig. 5** The images of golden plum during 6 days together with the proposed method results.

(a): the original images in six days; (b): the images of 'a' after background removal; (c): the H channel of 'b'; (d): the histogram of 'c'; (e): the quantized images of 'c'.

**Table 3** The percentage of each segment part for the images of Fig. 5.

Days	white	grey 1	grey 2	grey 3	black
1	98.07	0.70	0.48	0.32	0.36
2	97.92	0.80	0.50	0.35	0.43
3	96.53	1.98	0.65	0.36	0.48
4	95.98	2.28	0.81	0.41	0.52
5	93.10	5.02	0.88	0.47	0.53
6	68.91	25.80	4.06	0.69	0.54

Consequently, the obtained results show the feasibility of the suggested method and that it can

accurately illustrate the defected parts based on the degree of decay.

## 4. Conclusions

The development of digital color imaging gives the possibility of on-line quality control of agricultural and food products. In the present study, machine vision analysis was established for grading of some single color fruits. For this purpose, the images were captured with a RGB digital camera under diffuse illumination.



It was found that the best capturing angle was zero. HSV color space was found to be able to give superior results. It was shown that it is possible to remove the background using the S channel information. A histogram-based thresholding in the hue channel was employed for quantization and segmentation the images. The color change due to defect and aging is suitably distinguishable in H channel because of eliminating undesirable illuminating effects. Consequently, the fruit image can be precisely segmented based on the degree of defects, and it is possible to achieve the grade-cluster according to the percentage of each segment.

## References

- [1] T. Brosnan, D.W. Sun, Inspection and grading of agricultural and food products by computer vision systems: a review, *Computers and Electronics in Agriculture* 36 (2002) 193-213.
- [2] W.C. Lin, J.W. Hall, A. Klieber, Video imaging for quantify cucumber fruit color, *Hort. Tech.* 3 (4) (1993) 436-439.
- [3] Y. Tao, P.H. Heinemann, Z. Varghese, C.T. Morrow, H.J. Sommer, Machine vision for color inspection of potatoes and apples, *Trans. of ASAE* 38 (5) (1995) 1555-1561.
- [4] K.H. Choi, G.H. Lee, Y.J. Han, J.M. Bunn, Tomato maturity evaluation using color image analysis, *Trans. of ASAE* 38 (1) (1995) 171-176.
- [5] J.B. Njoroge, K. Ninomiya, N. Kondo, H. Toita, Automated fruit grading system using image processing, *Proc. SICE 2002*, Osaka, Japan, 2002, pp. 1346-1351.
- [6] M. Nagata, C. Qixin, Study on grade judgment of fruit vegetables using machine vision, *Japan Agricultural Research Quarterly* 32 (4) (1998) 257-265.
- [7] P. Yimyan, T. Chalidabhongse, P. Sirisomboon, S. Boonmung, Physical properties analysis of mango using computer vision, *Proc. of ICCAS2005*, Gyeonggi-Do, South Korea, 2005.
- [8] M.T. Riquelme, P. Bareiro, M. Ruiz-Altisent, C. Valero, Olive classification according to external damage using image analysis, *Journal of Food Engineering* 87 (2008) 371-379.
- [9] M. Zhang, L.I. Ludas, M.T. Morgan, G.W. Krutz, C.J. Precetti, Applications of color machine vision in the agricultural and food industries, *Proc. SPIE Vol. 3543*, Precision Agriculture and Biological Quality (1999) 208-219.
- [10] B.K. Miller, M.J. Delwiche, A color vision system for peach grading, *Trans. of ASAE* 32 (4) (1989) 1484-1490.
- [11] S. Nimesh, M.J. Delwiche, R.S. Johnson, Image analysis methods for real time color grading of stonefruit, *Comput. and Elec. in Agri.* 9 (1) (1993) 71-84.
- [12] F. Mendoza, P. Dejmek, J.M. Aquilera, Calibrated color measurements of agricultural foods using image analysis, *Postharvest Biology and Technology* 41 (2006) 285-295.
- [13] S. Somatilake, A.N. Chalmers, An image-based food classification system, *Proc. Image and Vision Computing New Zealand 2007*, Hamilton, New Zealand, December 2007, pp. 260-265.
- [14] R.S. Berns, Billmeyer and Saltzman Principles of Color Technology, 3<sup>rd</sup> ed., John Wiley & Sons, Inc., New York, 2000.
- [15] N. Ohta, A.R. Robertson, Colorimetry: Fundamentals and Applications, Chapter 4, John Wiley & Sons, Inc., New York, 2005.